

**NUMERICAL MODELING OF  
ONE-DIMENSIONAL OVERLAND FLOW OVER  
POROUS SURFACE**

**TAH AI SHER**

**UNIVERSITI SAINS MALAYSIA**

**2019**

**NUMERICAL MODELING OF  
ONE-DIMENSIONAL OVERLAND FLOW OVER  
POROUS SURFACE**

**By**

**TAH AI SHER**

**Thesis submitted in fulfilment of the  
requirements for the degree of  
Master of Science**

**May 2019**

## ACKNOWLEDGEMENT

It is my pleasure to be able to work alongside the people who have sincerely guided me in upholding both my practical, and theoretical skills in engineering and programming during my Master Studies. Firstly, I would like to thank Prof. Dr. Nor. Azazi Zakaria for encouraging me to believe in myself and for allowing me to pursue my interests by guiding me during my experience in the engineering environment of the real world.

Secondly, I would like to express my sincere appreciation to Dr. Puay How Tion for his constant guidance and encouragement. Furthermore, I want to thank him for always showing positive attitude towards my work, and for always giving his details replies towards my uncertainties in my entire theoretical question in my research.

Thirdly, I would like to thank my mentor, Mr. Low Koon Seng, for his unconditional support and knowledge regarding the real hydrological world experience. It would not have been possible for me to complete this study without his valuable encouragement. Furthermore, I want to give my sincere appreciation to Mr. Lim Jia Jun for his support and valuable guidance and to Mr. Muhammad Faiz Abdullah for his assistance on the experimental work throughout my research years.

I am sincerely grateful towards my parents, Mr. Tah Chung Keong and Madam Koh Moi Hon, as they are my inspiration and it is with their great support and continuous care in my life that has led me to become who I am today. To all of my sisters, Ms Tah Ai Wei, Ms. Tah Ai Lin, Ms Tah Ai Jenn and Ms Tah Ai Jia, thank you for the emotional and moral support. As to my husband, Mr. Chang Chin

How and my precious little girl, Chang Qi Anne, I would like to express my sincere gratitude for their unconditional love, trust and sacrifices in helping me to succeed in my studies.

In addition, I am sincerely grateful to my uncle, Mr Neoh Boon Hong, and my aunt, Madam Koh Mou Kiang, for their unconditional support and inspiration. To My father in law, Chang Huck Wah and my mother in law, Soh Cheng Khiaw, thank you for the great support along the way.

I would also like to give a special dedication to my beloved grandfather, Mr. Koh Boo Koh, for being one of my pillars and giving me the determination to succeed in life. Finally, I apologize to all whose names have been missed out but have also helped and supported me in various ways.

# TABLE OF CONTENT

<b>ACKNOWLEDGEMENT</b>	<b>ii</b>
<b>TABLE OF CONTENTS</b>	<b>iv</b>
<b>LIST OF TABLES</b>	<b>vii</b>
<b>LIST OF FIGURES</b>	<b>viii</b>
<b>LISTS OF SYMBOLS</b>	<b>xiii</b>
<b>ABSTRAK</b>	<b>xv</b>
<b>ABSTRACT</b>	<b>xvii</b>
<b>CHAPTER ONE: INTRODUCTION</b>	<b>1</b>
1.1 Background	1
1.2 Problem Statement	4
1.3 Research Objectives	6
1.4 Scope of Work	6
1.5 Limitation of Work	7
1.6 Dissertation Outline	7
<b>CHAPTER TWO: LITERATURE REVIEW</b>	<b>8</b>
2.1 Overview	8
2.2 The Sustainable Urban Drainage System (SuDS)	8
2.3 Numerical Modeling of SuDs	10
2.3.1 Infiltration model for flow over porous surface	11
2.3.2 Solving shallow water equation with higher-order scheme	13
2.4 Characteristics of first, second and third order numerical schemes	14

<b>CHAPTER THREE: METHODOLOGY</b>	<b>18</b>
3.1 Overview	18
3.2 Comparison of Different Numerical Scheme	20
3.3 Development of Numerical Model	22
3.3.1 Set Parameter	22
3.3.2 Set Initial Conditions of Flow Variable	23
3.4 Development of One-Dimensional Depth-Averaged Model	25
3.5 Numerical Algorithm	26
3.6 Verification of Numerical Model with Dam Break	29
3.7 Grid Convergence Test for Dam Break Flow Problem	30
3.8 Physical Model Experiment	31
3.8.1 Experimental Setup	31
3.8.2 Flume Model Assembly Process	34
3.9 Simulation of Flow over Porous Media	38
3.10 Summary	39
<b>CHAPTER FOUR: RESULTS AND DISCUSSION</b>	<b>40</b>
4.1 Overview	40
4.2 Comparison of Upwind Scheme with Exact Solution	40
4.3 Comparison of Central Scheme with Exact Solution	42
4.4 Comparison of Quadratic Upwind Interpolation for Convective Kinematics (QUICK) Scheme with Exact Solution	44
4.5 Comparison of Constrained Interpolation Scheme (CIP) with Exact Solution	47
4.6 One-Dimensional Dam Break Flow Problem	49

4.7	Grid Convergence Test for Dam Break Flow Problem	51
4.8	Validation of Numerical Simulation against with Experiment	52
4.9	Determination of Infiltration Rate	66
4.10	Propagation of Flow Front	70
4.11	Summary	74
 <b>CHAPTER FIVE: CONCLUSIONS AND RECOMMENDATIONS</b>		<b>75</b>
5.1	Conclusions	75
	5.1.1 To develop a one-dimensional numerical model with higher order scheme by solving the one-dimensional shallow water equation	75
	5.1.2 To include infiltration capability into the numerical model for the simulation of flow over porous media under unsaturated flow conditions	76
	5.1.3 To investigate the characteristics of flow over porous media	76
5.2	Recommendations for Future Research	77
 <b>REFERENCES</b>		<b>78</b>
 <b>APPENDIX A</b>		

## LIST OF TABLES

	<b>Page</b>
Table 1-1 Recommended runoff coefficients for various land uses (DID, 2012).	5
Table 3-1 Accuracy and features of different numerical schemes	20
Table 3-2 Simulate conditions for the advection of step function using different scheme	22
Table 3-3 Simulation condition of dam break flow problem	30
Table 3-4 Setup of numerical model for mesh convergence test	30
Table 3-5 Physical experiment set-up	33
Table 3-6 Simulation parameters for the numerical modeling of flow over porous media	38
Table 4-1 Result of the numerical simulation compared against physical experiment	52
Table 4-2 Discrepancy ratio between numerical and physical experimental data against length at time	52



## LIST OF FIGURES

	<b>Page</b>	
Figure 1-1	Schematic diagram of sponge city concept	2
Figure 1-2	Infiltration over porous media	3
Figure 2-1	Filter strips as a component in the SuDs system	10
Figure 2-2	Effect of dissipation and dispersion: (a) exact solution (b) numerical solution distorted primarily by dissipation errors (typical of first-order method), and (c) numerical solution distorted primarily by dispersion errors (typical of second-order method).	17
Figure 3-1	Overview of methodology	19
Figure 3-2	Solution algorithm for numerical model	24
Figure 3-3	Definition of flow parameters	26
Figure 3-4	Staggered mesh system diagram	27
Figure 3-5	Initial condition the one-dimensional dam break flow problem	30
Figure 3-6	Flume model	32
Figure 3-7	Experimental Setup (Side view)	32
Figure 3-8	Flume assembly process	35
Figure 3-9	Bracing the flume to make ensure constant width of the flume	35
Figure 3-10	Curing process	36
Figure 3-11	Relocating the flume	36
Figure 3-12	Constructing the dam gate slot	37
Figure 3-13	Side view of the actual physical model	37

Figure 3-14	Definition of impermeable and permeable zone in the numerical model	39
Figure 4-1	Numerical simulation of upwind scheme for (a) $t = 10.0s$ , (b) $t = 220.0s$ , (c) $t = 720.0s$ , (d) $t = 1240.0s$	41
Figure 4-2	Numerical simulation of central difference scheme at $t = 1.00s$	42
Figure 4-3	Numerical simulation of central difference scheme at $t = 10.00s$	43
Figure 4-4	Numerical simulation of central difference scheme at $t = 20.00s$	43
Figure 4-5	Numerical simulation of central difference scheme at $t = 40.00s$	44
Figure 4-6	Numerical simulation of QUICK scheme at $t = 0.01s$	45
Figure 4-7	Numerical simulation of QUICK scheme at $t = 0.10s$	45
Figure 4-8	Numerical simulation of QUICK scheme at $t = 0.25s$	46
Figure 4-9	Numerical simulation of QUICK scheme at $t = 0.60s$	46
Figure 4-10	Numerical simulation of CIP scheme at $t = 0.05s$	47
Figure 4-11	Numerical simulation of CIP scheme at $t = 0.40s$	48
Figure 4-12	Numerical simulation of CIP scheme at $t = 0.70s$	48
Figure 4-13	Numerical simulation of CIP scheme at $t = 1.40s$	49
Figure 4-14	Analytical and numerical solution for dam break flow over dry bed condition at (a) $t = 0.10s$ , (b) $t = 0.20s$ , (c) $t = 0.40s$ , (d) $t = 0.60s$ .	50
Figure 4-15	Grid Convergence Test	51
Figure 4-16	Numerical simulation (dotted) and experiment with 6mm beads (solid) at (a) $t = 0.2s$ , (b) $t = 0.4s$ , (c) $t = 0.6s$ , (d) $t = 0.8s$	54

	under condition of $h_o = 0.05\text{m}$	
Figure 4-17	Discrepancy ratio between numerical and experimental data against length at (a) $t=0.2\text{s}$ , (b) $t=0.4\text{s}$ , $t=0.6\text{s}$ and (d) $t=0.8\text{s}$ under condition of 6mm beads and $h_o = 0.05\text{m}$ .	55
Figure 4-18	Numerical simulation (dotted) and experiment with 6mm beads (solid) at (a) $t= 0.2\text{s}$ , (b) $t= 0.4\text{s}$ , (c) $t= 0.6\text{s}$ , (d) $t= 0.8\text{s}$ under condition of $h_o = 0.10\text{m}$	56
Figure 4-19	Discrepancy ratio between numerical and experimental data against length at (a) $t=0.2\text{s}$ , (b) $t=0.4\text{s}$ , $t=0.6\text{s}$ and (d) $t=0.8\text{s}$ under condition of 6mm beads and $h_o = 0.10\text{m}$ .	57
Figure 4-20	Numerical simulation (dotted) and experiment with 6mm beads (solid) at (a) $t= 0.2\text{s}$ , (b) $t= 0.4\text{s}$ , (c) $t= 0.6\text{s}$ , (d) $t= 0.8\text{s}$ under condition of $h_o = 0.15\text{m}$	58
Figure 4-21	Discrepancy ratio between numerical and experimental data against length at (a) $t=0.2\text{s}$ , (b) $t=0.4\text{s}$ , $t=0.6\text{s}$ and (d) $t=0.8\text{s}$ under condition of 6mm beads and $h_o = 0.15\text{m}$ .	59
Figure 4-22	Numerical simulation (dotted) and experiment with 10mm beads (solid) at (a) $t= 0.2\text{s}$ , (b) $t= 0.4\text{s}$ , (c) $t= 0.6\text{s}$ , (d) $t= 0.8\text{s}$ under condition of $h_o = 0.05\text{m}$	60
Figure 4-23	Discrepancy ratio between numerical and experimental data against length at (a) $t=0.2\text{s}$ , (b) $t=0.4\text{s}$ , $t=0.6\text{s}$ and (d) $t=0.8\text{s}$ under condition of 10mm beads and $h_o = 0.05\text{m}$ .	61
Figure 4-24	Numerical simulation (dotted) and experiment with 10mm beads (solid) at (a) $t= 0.2\text{s}$ , (b) $t= 0.4\text{s}$ , (c) $t= 0.6\text{s}$ , (d) $t= 0.8\text{s}$ under condition of $h_o = 0.10\text{m}$	62

Figure 4-25	Discrepancy ratio between numerical and experimental data against length at (a) $t=0.2s$ , (b) $t=0.4s$ , $t=0.6s$ and (d) $t=0.8s$ under condition of 10mm beads and $h_o = 0.10m$ .	63
Figure 4-26	Numerical simulation (dotted) and experiment with 10mm beads (solid) at (a) $t= 0.2s$ , (b) $t= 0.4s$ , (c) $t= 0.6s$ , (d) $t= 0.8s$ under condition of $h_o = 0.15m$	64
Figure 4-27	Discrepancy ratio between numerical and experimental data against length at (a) $t=0.2s$ , (b) $t=0.4s$ , $t=0.6s$ and (d) $t=0.8s$ under condition of 10mm beads and $h_o = 0.15m$ .	65
Figure 4-28	Accumulated volume losses with 6mm beads, $h_o = 0.05m$	67
Figure 4-29	Accumulated volume losses with 6mm beads, $h_o = 0.10m$	67
Figure 4-30	Accumulated volume losses with 6mm beads, $h_o = 0.15m$	68
Figure 4-31	Accumulated volume losses with 10mm beads, $h_o = 0.05m$	68
Figure 4-32	Accumulated volume losses with 10mm beads, $h_o = 0.10m$	69
Figure 4-33	Accumulated volume losses with 10mm beads, $h_o = 0.15m$	69
Figure 4-34	Propagation of flow front with porous bed of 6mm beads, $h_o = 0.05m$	71
Figure 4-35	Propagation of flow front with porous bed of 6mm beads, $h_o = 0.10m$	71
Figure 4-36	Propagation of flow front with porous bed of 6mm beads, $h_o = 0.15m$	72
Figure 4-37	Propagation of flow front with porous bed of 10mm beads, $h_o = 0.05m$	72
Figure 4-38	Propagation of flow front with porous bed of 10mm beads, $h_o = 0.10m$	73

Figure 4-39 Propagation of flow front with porous bed of 10mm beads, 73  
 $h_0 = 0.15\text{m}$

## LIST OF SYMBOL

$B$	Width of the channel
$d$	Diameter of beads
$F(t)$	Cumulative depth of infiltration
$g$	Gravitational acceleration
$h$	Flow depth
$h_0$	Initial water depth at reservoir
$h^*$	Temporary values for water depth after solving advection with CIP
$i$	Infiltration rate [m/s]
$K$	Saturated hydraulic conductivity
$n$	Manning's coefficient of roughness
$q_l$	Outflow discharge per unit length due to infiltration
$S_o$	Bed slope
$S_f$	Friction slope
$t$	Time [s]
$\Delta t$	Time step increment
$\tau_b$	Averaged bed shear stress
$U$	Depth-averaged velocity in $x$ -direction
$u^*$	Temporary values for velocity after solving advection with CIP
$\tilde{u}$	Temporary values for velocity prior to solving Poisson equation
$\Delta x$	Grid size in $x$ -direction
$x_{gate}$	Gate position
$\theta$	Water content

$\phi$  Arbitrary scalar or vector function

$\psi$  Suction head at the wetting front

# PEMODELAN BERANGKA ALIRAN DATARAN SATU DIMENSI DI PERMUKAAN BERLIANG

## ABSTRAK

Berikutan pembangunan yang pesat, sistem saluran permukaan air telah direkabentuk untuk bertindak sebagai saluran semulajadi seperti kawasan simpanan air yang membolehkan berlakunya proses penyerapan dan penyejatan. Tambahan pula, sistem ini dapat menyelesaikan isu-isu yang disebabkan oleh sistem perparitan tradisional. Oleh sebab terdapat permintaan yang tinggi dalam Sistem Saliran Bandar Mampan (*SuDs*) bagi menguruskan air ribut, satu model berangka mudah dan cekap untuk aliran di atas media berliang diperlukan. Tujuan penyelidikan ini ialah untuk membina sebuah model berangka untuk simulasi aliran di atas media berliang. Aliran permukaan tidak mantap dimodelkan dengan menggunakan persamaan air cetek satu dimensi. Ketepatan penyelesaian terma adveksi dalam persamaan momentum yang digunakan dalam penyelesaian berangka dapat ditingkatkan dengan menggunakan skim Profil Interpolasi Terkawal (CIP) yang mempunyai ketepatan taraf ketiga. Model berangka terdahulunya disahkan dengan menggunakan simulasi masalah aliran empangan pecah. Seterusnya, model berangka disahkan dengan perbandingan dengan eksperimen fizikal aliran empangan pecah di atas permukaan berliang. Hasil kajian mendapati bahawa prestasi model berangka ini memuaskan dari segi profil aliran permukaan dan kehilangan jumlah cecair melalui penyusupan. Kajian ini juga mendapati bahawa hubungan data eksperimen dan data berangka mempunyai persefahaman yang baik antara satu sama lain. Nisbah percanggahan antara data eskperimen dengan data berangka adalah di dalam lingkungan 0.716 hingga 1.031. Di samping itu, kajian mendapati bahawa hujung hadapan aliran menyebar di atas



permukaan berliang dengan kadar  $4/5$  terhadap masa. Hasil kajian ini dapat menyumbang kepada ketepatan yang lebih baik dalam permodelan berangka Sistem Saliran Bandar Mampan (SuDs).

# NUMERICAL MODELING OF ONE-DIMENSIONAL OVERLAND FLOW OVER POROUS SURFACE

## ABSTRACT

Due to rapid urbanization, surface water drainage systems are designed to perform as natural drainage acting as water storage areas that allow infiltration and evaporation. Furthermore, in order to solve issues caused by traditional drainage systems, there has been an increase of attention on Sustainable Urban Drainage systems (SuDs). Thus, to manage storm water, a simple yet efficient numerical model for flow over porous media is needed. The purpose of this research is to develop a numerical model for the simulation of flow over porous media. The model solves the unsteady one-dimensional shallow water equation. The accuracy of the numerical solution of the advection term in the momentum equation is increased by adopting the Constrained Interpolation Profile (CIP) scheme which is of the third order accuracy. The numerical model was firstly verified by simulating the dam-break flow problem. It was then validated against physical experiment of dam-break flow over porous bed. The author found that the numerical model performed satisfactorily in terms of surface flow profile and the loss of volume of flow through infiltration. This study found that the relationship of experimental data and numerical data has good agreement between each other with a discrepancy ratio of experimental data over numerical data ranging from 0.716 to 1.031. Besides, the flow front propagation is proportional to time with the  $4/5$  exponent power of ( $l \propto t^{4/5}$ ). The outcome of this study can help to provide better accuracy when designing a sustainable urban drainage system (SuDs) with porous media.

## CHAPTER ONE

### INTRODUCTION

#### 1.1 Background

Urbanization and the changes of land use is one of the causes of flash flood. This is due to the increase in the impervious surface. In the event of a heavy rainfall, the area affected will have a large surface runoff volume which will flow quickly into the drainage system. This is due to the lack of interception, infiltration and storage at site. With the ever increasing storm intensity due to climate change, the existing conventional drainage system will be put under stress, increasing the risk of flash flood and prolong inundation in urban areas.

The Sustainable Urban Drainage System (SuDs) is a surface water drainage scheme designed to perform like natural drainage system by promoting infiltration and evaporation process. The SuDS also provides areas to store water by allowing infiltration to ground water, thus proving a better way to solve inundation related issues as compared with the traditional drainage system (Marchioni and Becciu, 2010). Of late, we see the implementation of the SuDs in China on a large scale called the Sponge City Concept as shown in Fig. 1-1 (Hydrolink, 2016). This concept is based on six principal guidelines, which are infiltrate, detain, store, cleanse, use and drain. It is not only for flood control but also rainwater harvesting, improving the water quality and restoring the ecology as well. It adopts and adapts the USA low impact development approach, coupled with grey infrastructure, a necessary characteristic needed for dealing with more significant flood events.

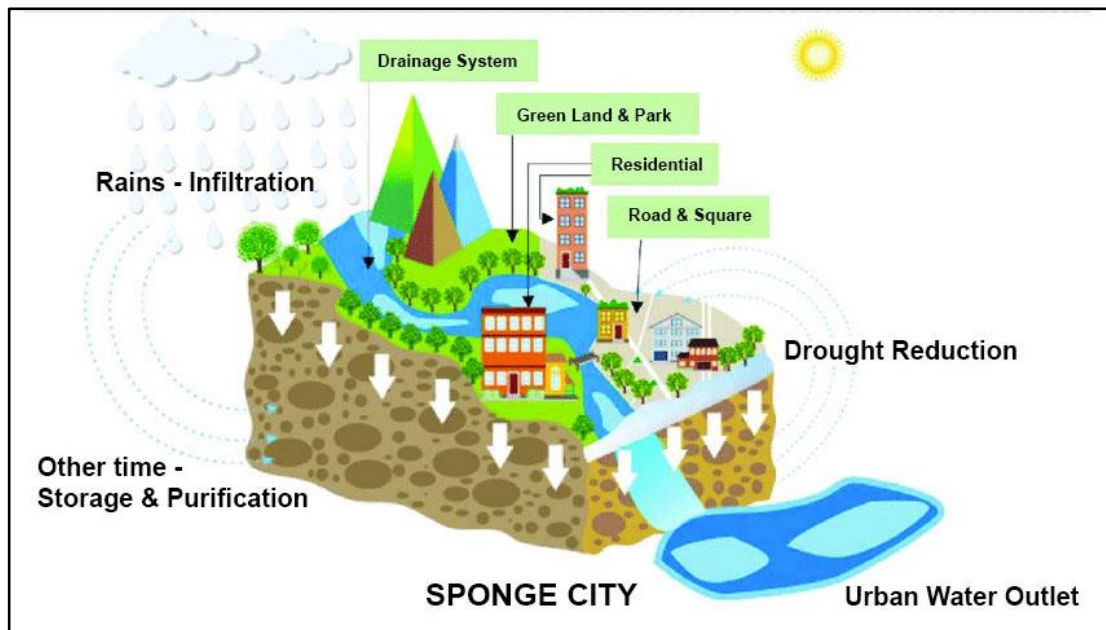


Figure 1-1: Schematic diagram of sponge city concept (Chan et al., 2018).

There are 4 main pillars contributing to Sustainable Urban Drainage Systems (SuDs). These pillars are:

- a) water quantity which leads to flooding issue.
- b) water quality which leads to pollution issue.
- c) biodiversity which leads to the wildlife and plants issue.
- d) amenities which are related to the quality of life in our society.

The first two main pillars, (a) and (b), are being realized by a primarily physical process: *infiltration of flow*. Infiltration processes of surface water into subsurface media can be seen in most SuDs facilities. For example, green roof allows rainwater to be infiltrated into planted soil layer, filter strips, filter drain while swales allow flows to infiltrate as it travels on the surface, thus allowing ground water to be recharged. In some cases, infiltrated flow is stored in underground storage systems before being channelled out to discharge point. The pervious pavement used in car parks and highways also allow infiltration of surface flow for the purpose of reducing peak flow and improving water quality.

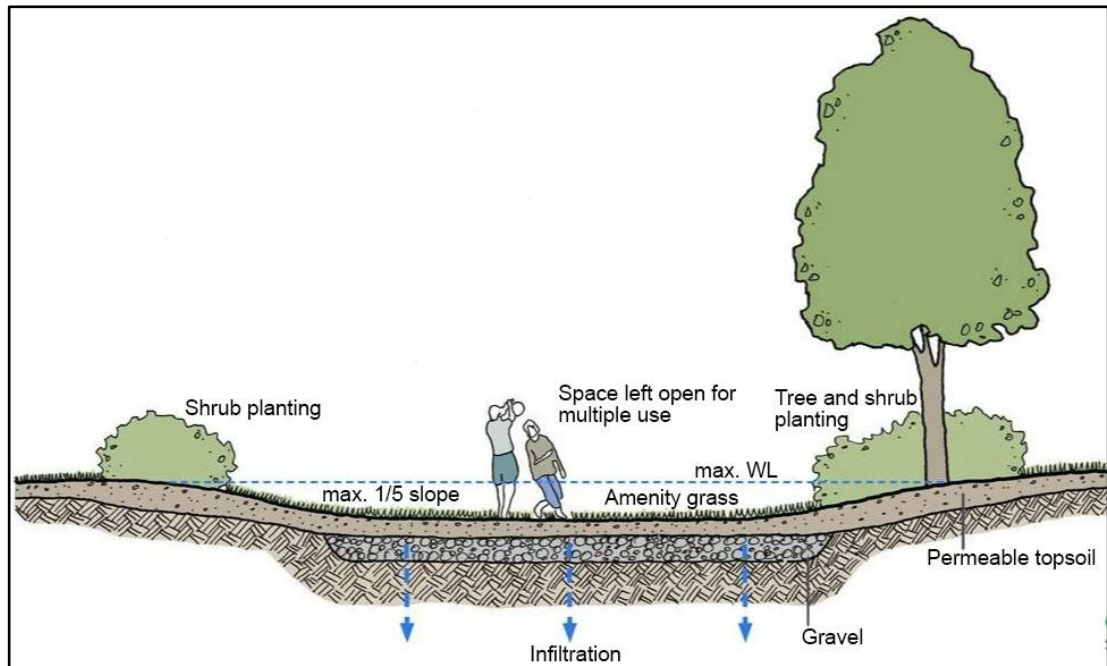


Figure 1-2: Infiltration process in a detention basin (Susdrain, 2000).

If space is plenty, detention basins are used as storm runoff storage. During dry periods, the detention basins can be used for amenity purposes such as being used as a playground, as shown in Fig. 1-2.

Nowadays, water resource management has become the main source of concern due to extensive urbanization and climate change. With the help of modern technology, computerised models using innovative approaches are being designed in order to help efficiently design Sustainable Urban Drainage Systems (SuDs). This is to optimize and meet environmental and economic preconditions (Karl, 2015).

In this study, a mathematical model is developed using one-dimensional depth-averages with higher order schemes in order to simulate flow over porous media which is used to represent the previous subsurface condition. To increase the accuracy of the numerical model, a third order numerical scheme, i.e. Constrained Interpolation Profile (CIP) (Yabe et al., 2004) scheme, is adapted in this model to solve the advection term in the momentum equation. The numerical model is first

verified against the one-dimensional dam break problem of inviscid fluid. The numerical model is then used to simulate flow over porous media, by releasing a finite volume of water retained behind a gate onto porous bed. The infiltration rate is determined through experiments and used in the numerical model. The performance of the numerical model is validated against experimental results in terms of the reproduction of water surface profile

## **1.2 Problem Statement**

In Malaysia, the current trend of storm water management is based on Urban Stormwater Management Manual for Malaysia (MSMA), 2<sup>nd</sup> edition. Drainage design practice for the estimation of runoff based on land area smaller than 80 hectare, the Rational Method: CIA method (coefficient of runoff, intensity of rainfall and Area of catchment) is used. For land areas larger than 80 hectares, the Time-Area method is used, by utilizing the rainfall excess hyetograph with time area diagram where isochrones method is used.

Since both are using the lump method, the models are unable to describe the temporal changes of the flow in space. Furthermore, the design is not economical for large scale developments and this lump method design does not give any spatial infiltration of flow as well. The Rational method uses runoff coefficients to cater for the effect of infiltration (DID, 2012). For example, the runoff coefficient for various land use is shown in Table 1-1. Meanwhile when the Time Area Method is used, the infiltration of surface runoff is assumed to be constant or decreasing without the consideration of soil porosity.

In Urban Stormwater Management Manual for Malaysia (MSMA), pavement drainage was discussed under chapter 13 (DID, 2012). However, the design of

porous pavement drainage designs and guidelines information is insufficient. Therefore, a numerical model can be used for more efficient design of SuDs component. This is due to the fact that a numerical model provides accurate temporal and space solution for the flow. Based on the results from the numerical model, a better guideline for SuDs design can be established.

Table 1-1: Recommended runoff coefficients for various land uses (DID, 2012).

Landuse	Runoff Coefficient (C)	
	For Minor System ( $\leq 10$ year ARI)	For Major System ( $> 10$ year ARI)
<b>Residential</b>		
Bungalow	0.65	0.70
Semi-detached Bungalow	0.70	0.75
Link and Terrace House	0.80	0.90
Flat and Apartment	0.80	0.85
Condominium	0.75	0.80
<b>Commercial and Business Centres</b>	0.90	0.95
<b>Industrial</b>	0.90	0.95
<b>Sport Fields, Park and Agriculture</b>	0.30	0.40
<b>Open Spaces</b>		
Bare Soil (No Cover)	0.50	0.60
Grass Cover	0.40	0.50
Bush Cover	0.35	0.45
Forest Cover	0.30	0.40
<b>Roads and Highways</b>	0.95	0.95
<b>Water Body (Pond)</b>		
Detention Pond (with outlet)	0.95	0.95
Retention Pond (no outlet)	0.00	0.00

### **1.3 Research Objectives**

The objectives of this study are as follows:

- a) To develop a one-dimensional numerical model with higher order scheme by solving the one-dimensional shallow water equation.
- b) To include infiltration capability in the numerical model for the simulation of flow over porous media under unsaturated flow conditions.
- c) To investigate the characteristics of flow over porous media.

### **1.4 Scope of Work**

In this research, tasks carried out are to have more in-depth understanding and to understand the characteristic of different numerical schemes in solving advection equation to justify the decision to adapt higher order schemes for the numerical modelling. The development of the numerical modelling includes discretizing the partial differential equations with the inclusion of Manning's  $n$  and infiltration rate.

Some experimental works were conducted at the hydraulic lab of River Engineering and Urban Drainage Research Center (REDAC), Universiti Sains Malaysia. A physical rectangular tank was built for the simulation of dam-break flow over porous media with three different water depths, i.e., 0.05m, 0.10m, 0.15m. The porous zone is made up of two different single size glass beads, i.e., 6mm and 10mm. Then, the infiltration rate data obtained from experiment was used to verify the numerical modelling data. The data were compared with numerical modelling simulation, physical model data and literature review data from other researchers.



## 1.5 Limitation of Work

In this study, there are some limitations such as:

- a. Constant infiltration rate was assumed in the numerical model.
- b. Constant coefficient of Manning's  $n$  was assumed in the numerical model.

## 1.6 Dissertation Outline

Outlines of the dissertation are shown below:

**Chapter 1** describes the overview of the research which includes the background of the research, problem statement, objectives, and scopes of work and dissertation outline.

**Chapter 2** reviews the literature of the research. Studies carried out by other researchers are being reviewed to relate with this research.

**Chapter 3** explains the methodology of the research which includes the theories, experiments and applications of the numerical model.

**Chapter 4** shows the results and discussions of this research. The results of the numerical simulation and experiment on the physical model are compared and justified.

**Chapter 5** concludes the outcome of this research and provides recommendation for future work.

## **CHAPTER TWO**

### **LITERATURE REVIEW**

#### **2.1 Overview**

The Sustainable Urban Drainage System (SuDs) is an alternative approach to urban storm water management. SuDs manage the surface runoff by attenuation of peak flow and the reduction total runoff volume. Section 2.2 discusses the features and characteristics of SuDs along with the designing guidelines. The numerical modeling of SuDs is crucial in determining the most suitable model. Section 2.3 discusses the numerical model developed in previous studies. In addition, various studies conducted with the incorporation of infiltration model are also being discussed. By improving the accuracy of numerical schemes, researchers are adopting higher order schemes in order to solve the shallow water equations. Section 2.4 discusses the characteristics of numerical schemes with different orders.

#### **2.2 The Sustainable Urban Drainage System (SuDs)**

The Sustainable Urban Drainage System, or more widely known as SuDs, is a rather new approach to urban storm water management. In order to create a green and sustainable infrastructure to manage urban storm water with additional advantages in promoting biodiversity and amenity to urban dwellers, the SuDs design and approach revolves around low impact and low energy control.

Several components, which were installed in a treatment-train style in SuDs, are implemented to manage the quantity and quality of the stormwater. Filter strips are one of the examples found in treatment train style where it is installed besides the road shoulder at the first stage to improve the removal of sediments and increase the

attenuation of peak flow before the runoff is diverted into a swale for conveyance and storage purposes as shown in Fig. 2-1. The runoff from the swale is then channeled into a bio-detention pond for water quality treatment.

SuDs manage the surface runoff through attenuation of peak flow and reduction total runoff volume. This is achieved by the following methods (CIRIA, 2016) :

- a) Allowing surface runoff to infiltrate through permeable surfaces and return to groundwater.

Example: rain garden, soakaways, infiltration trenches, infiltration basins, infiltration blankets and wet swale

- b) Allowing surface runoff to infiltrate through permeable surface and stored temporarily on surface or underground. Infiltration into groundwater is allowed.

Example: bio-retention, attenuation storage tanks and pervious pavement

- c) Allowing surface runoff to infiltrate through permeable surface, while at the same time conveyed to next treatment stage. Infiltration into groundwater is allowed (if unlined).

Example: dry swale and filter strip such as dry swale can be combined with underground temporary storage (Zakaria et al. 2011).

When designing SuDs components such as the filter strip, filter drain, permeable pavement, swale, green roofs and swales, calculation or estimation of the flow depth, propagation speed, and residence time in the component is critical. Sizing and designing of the capacity of these components depend on flow depth and resistance

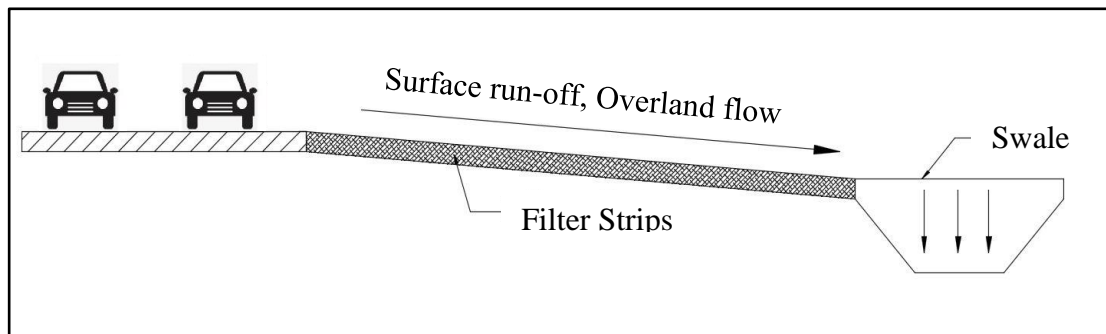


Figure 2-1: Filter strips as a component in the SuDs system.

time. Thus, an estimation of flow hydrograph along the treatment train is important to avoid bottleneck and overflow due to design failure.

### 2.3 Numerical Modeling of SuDs

Hortonian overland flow in SuDs components such as filter-strip, green roofs and permeable pavement. Hortonian overland flow (identical to overland flow) occurs when the intensity of the rainfall exceed the rate at which water can infiltrate the ground in an area and the excess water accumulates on the soil's surface and starts moving downslope due to gravity. (Encyclopedia of Agrophysics, 2011).

In general, overland flow demonstrates nearly horizontal free-surface profile with very small or negligible curving and vertical acceleration. Therefore, the pressure distribution can be assumed to be hydrostatic which can be adequately described by using shallow water equations (Chanson, 2004). The application of shallow water equations for mathematical and numerical studies of overland flow is widely used and can be seen in the work of Hou et al. (2018), Shih (2018), Singh (2017), Liang et al. (2015), Cea et al. (2010) Liu et al (2004) and Yang (2016) can be traced back to much earlier work of Akan (1981), Smith et al (1971) and Woolhiser et al (1967). Hou et al (2018) solved the full dynamic shallow equations in their

studies of overland flows. Meanwhile, Singh (2017), Akan (2016, 2013, 1981), Liu et al. (2004), Woolhiser (1996, 1967) and Smith et al. (1971) adopted the kinematic wave equations, which are derived and simplified from the shallow water equations. Rujner et. al (2018) in their study of grass swale response to high inflow of runoff with a proprietary software Mike-SHE, has opted the diffusive wave approximation of the shallow water equation.

As the fully-dynamics, diffusive wave or kinematic wave approximation have differences are derived based on different assumptions (Miller, 1984), especially diffusive and kinematic wave. The choice of form for the governing equations depends on the purpose of the study as the flow features to be investigated and the numerical solution techniques to be applied. One of the advantages of using the kinematic wave equation is the availability of analytical solutions (Jain, 2001). On the other hand, the fully-dynamics shallow water equation allows reproduction of such as backwater effects, pressurized flow conditions and estimation of dynamic forces.

### **2.3.1 Infiltration model for flow over porous surface**

Most SuDs components depend on permeable surfaces for flow attenuation and reduction of runoff volume through infiltration process (CIRIA, 2016), the determination of infiltration rate and its relationship with the surface flow condition is a critical factor in accurate mathematical and numerical modeling of flow over a permeable surface or porous surface.

Infiltration rate on a porous surface depends on the soil type and condition (which affect porosity, capillary force and adsorption), soil antecedence moisture

content, ground water level, flow depth on the surface (therefore the rainfall intensities) as well as slope and vegetation on the surface (Subramanya, 2013). In numerical modeling of flow over porous surface, there are several approaches to model the infiltration process. The adoption of time dependent infiltration model such as the Green-Ampt equation can be seen in the work of Akan (2016), Chen et al. (2016) and Stone et. al. (1992). The Green- Ampt model can derived from the Darcy equation and it is often expressed in cumulative depth of infiltration  $F(t)$  which is a function of suction head at the wetting front  $\psi$  , water content  $\theta$  , hydraulic conductivity  $K$  and time  $t$  as given in the following equation (Mays, 2010),

$$F(t) = Kt + \psi\Delta\theta \ln \left[ 1 + \frac{F(t)}{\psi\Delta\theta} \right] \quad (2.1)$$

However, the Green-Ampt model disregard the role of surface water depth on the infiltration rate as can be seen in Eq. (2.1) (Yang, 2016).

Coupling of surface flow with subsurface flow is another alternative to model the infiltration process. The momentary infiltration rate which depends on the flow depth was used by Smith and Woolhiser (1971) where the one-dimensional surface flow model is combined with a one-dimensional subsurface model. Therefore, the subsurface model only considered the vertical movement of flow. Akan et. al (1981) further improved the subsurface model to allow two-dimensional subsurface flow by coupling the one-dimensional surface flow model with the two-dimensional subsurface model in the determination of infiltration rate on the surface. Woodhiser et al. (1996) adopted the one-dimensional surface and two-dimensional subsurface coupling with the Smith-Parlange equation used for the infiltration rate. Ying et al.

(2016) used the semi-analytical approach to determine the sorptivity  $S$  term in Philip's infiltration rate equation expressed in the following equations,

$$i = \frac{1}{2} S t^{-0.5} \quad (2.2)$$

where  $i$  is the infiltration rate and  $t$  is time.

On the other hand, Hou et al. (2018) used constant infiltration rate based on land used in the calibration process for the simulation of rainfall-runoff process in Wangmaogao catchment in the Shaanxi Province of China.

### **2.3.2 Solving shallow water equation with higher-order scheme**

The accuracy of numerical schemes can be achieved by adopting higher order scheme. The first order scheme, although very stable, tends to be very dissipative and thus, could not capture discontinuities and shocks (Anderson et al. 2016). However, the higher order scheme often comes with dispersion errors. The Godonuv's method is often used to develop higher order schemes and limiters are often used to suppress the dispersion errors (Anderson et al. 2016). Alcurdo et al. (1993) adopted a high-resolution Godonuv-type scheme to solve the two-dimensional shallow water equations, with the application MUSCL method. Ouyang et al. (2013) used the finite-difference MacCormack method with total variation diminishing property (TVD) to simulate debris flow with second order accuracy in time and space. Another method based on WENO scheme of fifth order is used by Li et al. (2015) to simulate shallow flow. The WENO scheme is non-oscillatory near discontinuities.

A semi-Lagrangian method based on the method of characteristics (MOC) is used by Erbes (1993) to solve the one-dimensional shallow water equations. The MOC method is also adopted in some proprietary software such as HEC-RAS and

SOBEK (Shih et al. 2018). Based on the MOC method, Akoh et al. (2008) and Yabe and Ogata (2010) applied the third order accuracy Cubic Interpolation Profile (CIP) interpolation, to solve the shallow water equations. On the other hand, Kawasaki et al. (2015) applied the CIP scheme to solve the shallow water equation for the simulation of tsunami run-up without using the MOC method. The Kawasaki and Kozuki (2015) method is based on finite difference in Eulerian grid, and therefore easier to apply compared to the MOC method adopted by Akan et al. (2008) and Yabe and Ogata (2010).

#### 2.4 Characteristics of first, second and third order numerical schemes

The one-dimensional shallow water equations, also known as the Saint-Venant equations are often used to describe unsteady open channel flow. It is comprised of the continuity and momentum equations, expressed as follows (Chanson, 2004):

$$\begin{array}{l} \text{Continuity} \\ \text{equation:} \end{array} \quad \frac{\partial h}{\partial t} + U \frac{\partial h}{\partial x} + h \frac{\partial U}{\partial x} = 0 \quad (2.3)$$

$$\begin{array}{l} \text{Momentum} \\ \text{equation:} \end{array} \quad \frac{\partial U}{\partial t} + U \frac{\partial U}{\partial x} + g \frac{\partial h}{\partial x} = g(S_o - S_f) \quad (2.4)$$

Here,  $U$  is the depth-averaged velocity in  $x$ -direction.  $h$  is the flow depth,  $g$  is gravitational acceleration,  $S_o$  is the bed slope and  $S_f$  is the friction slope. The first two terms on the left hand side of momentum equations is the advection term and it is a non-linear hyperbolic equation (Yabe and Aoki , 1991). The accuracy of the solution of non-linear hyperbolic equation (also known as the Burger's equation) depends on the order of the numerical schemes (Anderson et al., 2016).



### Numerical solution of wave equation

The first order wave equation is expressed as follows,

$$\frac{\partial \phi}{\partial t} + c \frac{\partial \phi}{\partial x} = 0 \quad (2.3)$$

Here  $\phi$  is any scalar or vector properties to be advected with constant velocity  $c$ . Eq. (2.3) is the linear hyperbolic equation. It can be easily solved with numerical method as follows,

#### First order upwind scheme,

Eq. 2.3 can be discretized using the first order upwind scheme as follows:

$$\begin{aligned} \phi_j^{n+1} = \phi_j^n - \frac{1}{2}(v_{CFL} + |v_{CFL}|)(\phi_j^n - \phi_{j-1}^n) \\ - \frac{1}{2}(v_{CFL} - |v_{CFL}|)(\phi_{j+1}^n - \phi_j^n) \end{aligned} \quad (2.4)$$

Where  $v_{CFL} = c\Delta t/\Delta x$ ,  $\phi_j^n$  is the value of  $\phi$  at grid location  $j$  at time step  $n$  and  $\phi_j^{n+1}$  is the value of  $\phi$  at grid location  $j$  at time step  $n + 1$  (at time  $t + \Delta t$ ).  $\Delta t$  is the time step increment and  $\Delta x$  is the grid size. As the scheme is first order in space, it is subjected to primarily dissipation error due to numerical viscosity effect (Anderson et al., 2016) as shown in Figure 2-2.

### Second order central difference scheme

Eq. 2.3 can be also discretized using the central difference scheme which is of second order accuracy as follows:

$$\phi_j^{n+1} = \phi_j^n - \frac{1}{2}(v_{CFL})(\phi_{j+1}^n - \phi_{j-1}^n) \quad (2.5)$$

The numerical solution of the second order central difference scheme is primarily distorted by dispersion errors as shown in Fig. 2-2 (Anderson et al., 2016).

### Third order QUICK scheme

By using the third order QUICK scheme, Eq. 2.3 can be discretized as follows,

$$\begin{aligned} \phi_j^{n+1} &= \phi_j^n - \frac{1}{8}v_{CFL}(3\phi_{j+1}^n + 3\phi_j^n - 7\phi_{j-1}^n + \phi_{j-2}^n) & \text{For } c \geq 0 \\ \phi_j^{n+1} &= \phi_j^n - \frac{1}{8}v_{CFL}(-3\phi_{j-1}^n - 3\phi_j^n + 7\phi_{j+1}^n - \phi_{j+2}^n) & \text{For } c < 0 \end{aligned} \quad (2.6)$$

The QUICK scheme suffers from undershoot and overshoot problem (Neumann, 2011).

### Third order CIP scheme

The CIP scheme was developed by Yabe et al. (1985). CIP stands for Cubic Interpolated Pseudo Particle or Constrained Interpolation Profile. The CIP scheme uses the advection scalar or vector value and its spatial gradient to solve the third order interpolation polynomial. By using CIP scheme, Eq. 2.3 can be solved as follows,

$$\phi_i^{n+1} = a_i\xi^3 + b_i\xi^3 - (\phi')_i^n\xi + \phi_i^n \quad (2.7)$$

$$(\phi')_i^{n+1} = 3a_i\xi^2 + 2b_i\xi + (\phi')_i^n \quad (2.8)$$

where  $\xi = -\Delta t \cdot u$ ,  $(\phi')_i^{n+1} = \frac{\partial \phi}{\partial x}$  = gradient of  $\phi$  at point  $i$ , while  $a_i$  and  $b_i$  are coefficient to be determined.

It is with the note that, the CIP scheme can be used to solve the non-linear hyperbolic equation which appears in the shallow water momentum equation in Eq. 2.4 with third order accuracy. It has been shown to be able to capture discontinuity and shock waves well (Yabe et al. 1985, Yabe et al. 1991).

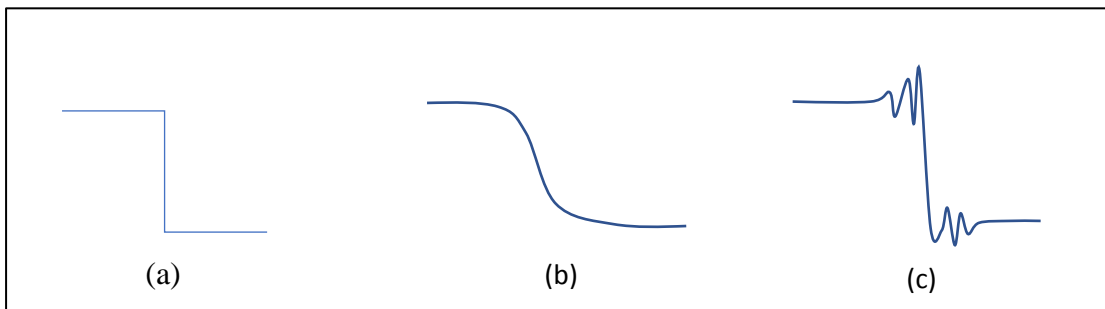


Figure 2-2: Effect of dissipation and dispersion: (a) exact solution (b) numerical solution distorted primarily by dissipation errors (typical of first-order method), and (c) numerical solution distorted primarily by dispersion errors (typical of second-order method) (Anderson et al., 2016).

## **CHAPTER THREE**

### **METHODOLOGY**

#### **3.1 Overview**

This chapter describes the methodology of this research. This research is conducted in two parts as shown in Fig. 3-1.

Part A: Solving the advection equation and comparing different numerical scheme performance to decide on the best scheme to be implemented for this study. These schemes are the first, second and third order schemes.

Part B: Adopting the higher order scheme in numerical simulation and verification of the model with the dam break flow problem. A mesh convergence test is carried out to determine the most economical grid size. As for the physical experiment section, a physical model is built to obtain the infiltration rate over the porous media. By obtaining the infiltration rate data from the physical experiment, it is fed into the numerical model. The numerical model is validated against the physical experiment, by comparing the flow profiles. Furthermore, an observation of the flow characteristic of front propagation from the experiment and numerical model is conducted.

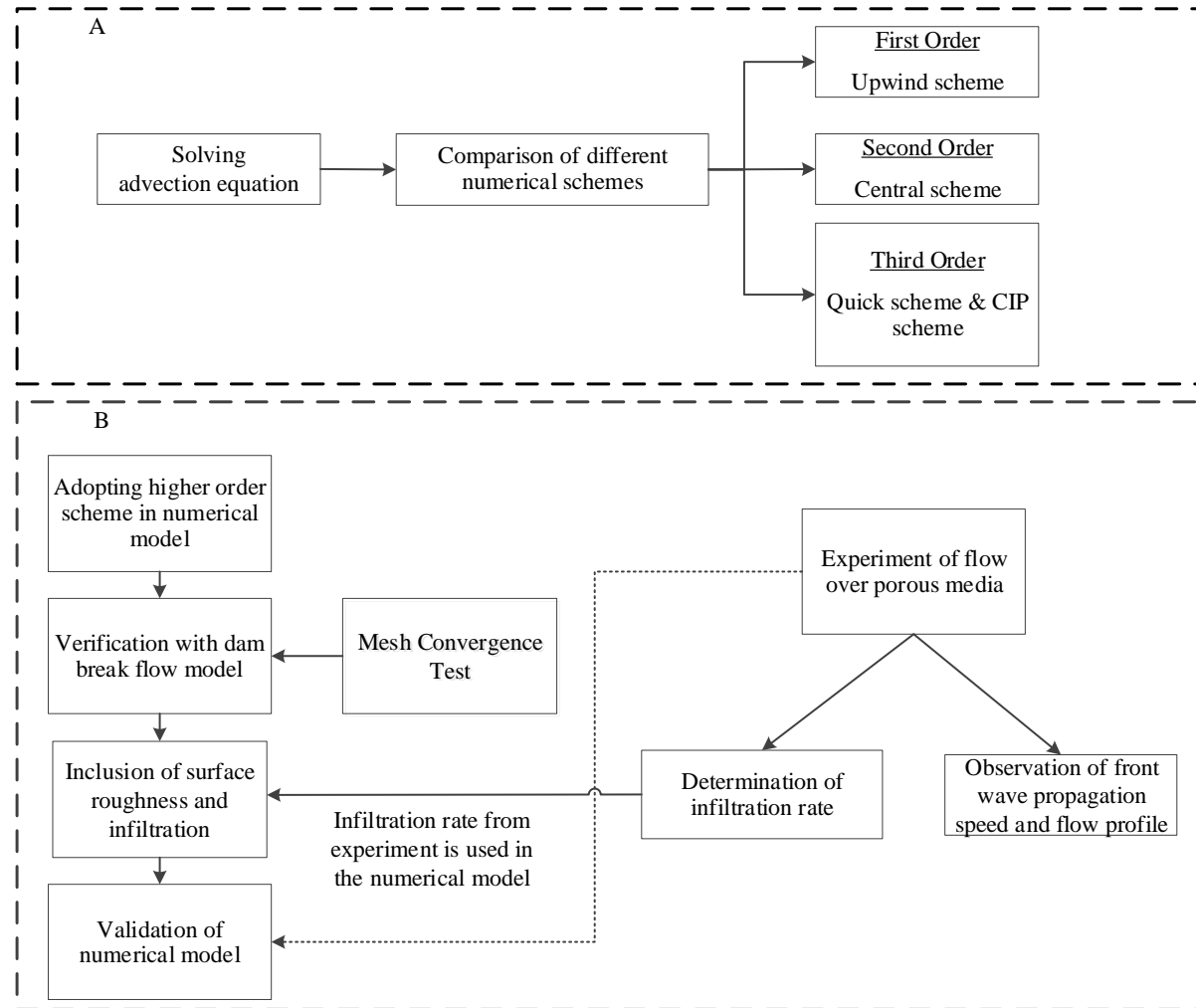


Figure 3-1: Overview of methodology.

Table 3-1: Accuracy and features of different numerical schemes.

Scheme	Accuracy	Features
Upwind	First order	Easy to implement, however primarily subjected to dissipation error.
Central	Second order	Higher accuracy, however primarily subjected to dispersion error.
Quick	Third order	Higher accuracy, however more cell information is needed and local extrema occur at discontinuity.
CIP	Third order	Higher accuracy and compact (using variable value and its spatial value)

### 3.2 Comparison of Different Numerical Scheme

The application of CIP scheme for shallow water equations is described earlier in Chapter 2, Section 2.3.2. Furthermore, a comparison of different schemes is shown in Table 3-1 as a summarized of the scheme features.

The accuracy and performance of different numerical schemes in solving the advection equation is carried out in this section. The advection equation for scalar quantity  $\phi$  with constant velocity  $u$  is given as follows,

$$\frac{\partial \phi}{\partial t} + u \frac{\partial \phi}{\partial x} = 0 \quad (3.1)$$

A step function is used as initial condition for  $\phi$ . The step function initial condition is described mathematically in Eq. 3.2. The velocity field is given as in Eq. 3.3.

$$\phi(x, 0) = \begin{cases} 1.0, & 50m \leq x \leq 150m \\ 0.0, & \text{others} \end{cases} \quad (3.2)$$

$$u(x, t) = 1.0 \text{ m/s} \quad (3.3)$$

**a) First order upwind scheme**

Eq. 3.1 is discretized using the first order upwind scheme as follows,

$$\phi_i^{n+1} = \begin{cases} \phi_i^n - \Delta t u_i \frac{\phi_i^n - \phi_{i-1}^n}{\Delta x}, & u_i \geq 0 \\ \phi_i^n - \Delta t u_i \frac{\phi_{i+1}^n - \phi_i^n}{\Delta x}, & u_i < 0 \end{cases} \quad (3.4)$$

**b) Second order central scheme**

Eq. 3.1 is discretized using the second order central scheme as follows,

$$\phi_i^{n+1} = \phi_i^n - \Delta t u_i \frac{\phi_{i+1}^n - \phi_{i-1}^n}{2\Delta x} \quad (3.5)$$

**c) Third order Quadratic Upwind Interpolation for Convective Kinematics (QUICK) scheme**

Eq. 3.1 is discretized using the third order QUICK scheme as follows,

$$\phi_i^{n+1} = \begin{cases} \phi_i^n - \Delta t u_i \frac{3\phi_{i+1}^n + 3\phi_i^n - 7\phi_{i-1}^n + \phi_{i-2}^n}{8\Delta x}, & u_i \geq 0 \\ \phi_i^n - \Delta t u_i \frac{3\phi_{i-1}^n - 3\phi_i^n + 7\phi_{i+1}^n - \phi_{i+2}^n}{6\Delta x}, & u_i < 0 \end{cases} \quad (3.6)$$

**d) Third order Constrained Interpolation Scheme (CIP) scheme**

Eq. 3.1 is discretized using the third order CIP scheme as follows,

$$a_i = \frac{\phi'_i + \phi'_{i-1}}{\Delta x^2} - 2 \frac{\phi_i - \phi_{i-1}}{\Delta x^3} \quad (3.7)$$

$$b_i = 3 \frac{\phi_i - \phi_{i-1}}{\Delta x^2} - \frac{\phi'_i - 2\phi'_{i-1}}{\Delta x} \quad (3.8)$$

$$\phi_i^{n+1} = a_i \xi^3 + b_i \xi^2 - (\phi')_i^n \xi + \phi_i^n \quad (3.9)$$

$$(\phi')_i^{n+1} = 3a_i \xi^2 + 2b_i \xi + (\phi')_i^n \quad (3.10)$$

For the numerical solution of the advection of step function using the first order upwind, second order central, third order QUICK and third order CIP schemes, the setup for simulations are shown in Table 3-2. Whereby, the results are shown in Chapter 4, Section 4.1 to Section 4.4.

Table 3-2: Simulate conditions for the advection of step function using different scheme.

Parameters	Upwind scheme	Central scheme	QUICK scheme	CIP scheme
Cell size, $\Delta x$ [m]	2.0	2.0	2.0	2.0
Time interval, $\Delta t$ [s]	0.1	0.1	0.1	0.1
Velocity, $u$ [m/s]	1.0	1.0	1.0	1.0
Domain size [m]	10 000	500	500	500

### 3.3 Development of Numerical Model

The numerical model is coded in Fortran language to develop a numerical model to simulate the flow along with manning's  $n$  and infiltration.

The solution algorithm for the numerical model is shown in Fig. 3-2 with detailed explanation. This study also shows an increase of accuracy of the numerical model by integrating higher order CIP numerical scheme which will be discussed further in section 3.4.

#### 3.3.1 Set Parameters

Firstly, all simulation parameters are set according to the conditions such as:

- a) Mesh size is designated as  $\Delta x$  [m]
- b) Time interval is designated as  $\Delta t$  [s]
- c) Infiltration rate result as  $q_l$ , [ $m^2/s$ ]



### **3.3.2 Set Initial Conditions of Flow Variable**

The initial conditions for the variable velocity,  $u$  and initial depth,  $h_0$  of the numerical model is set up accordingly based on the condition.

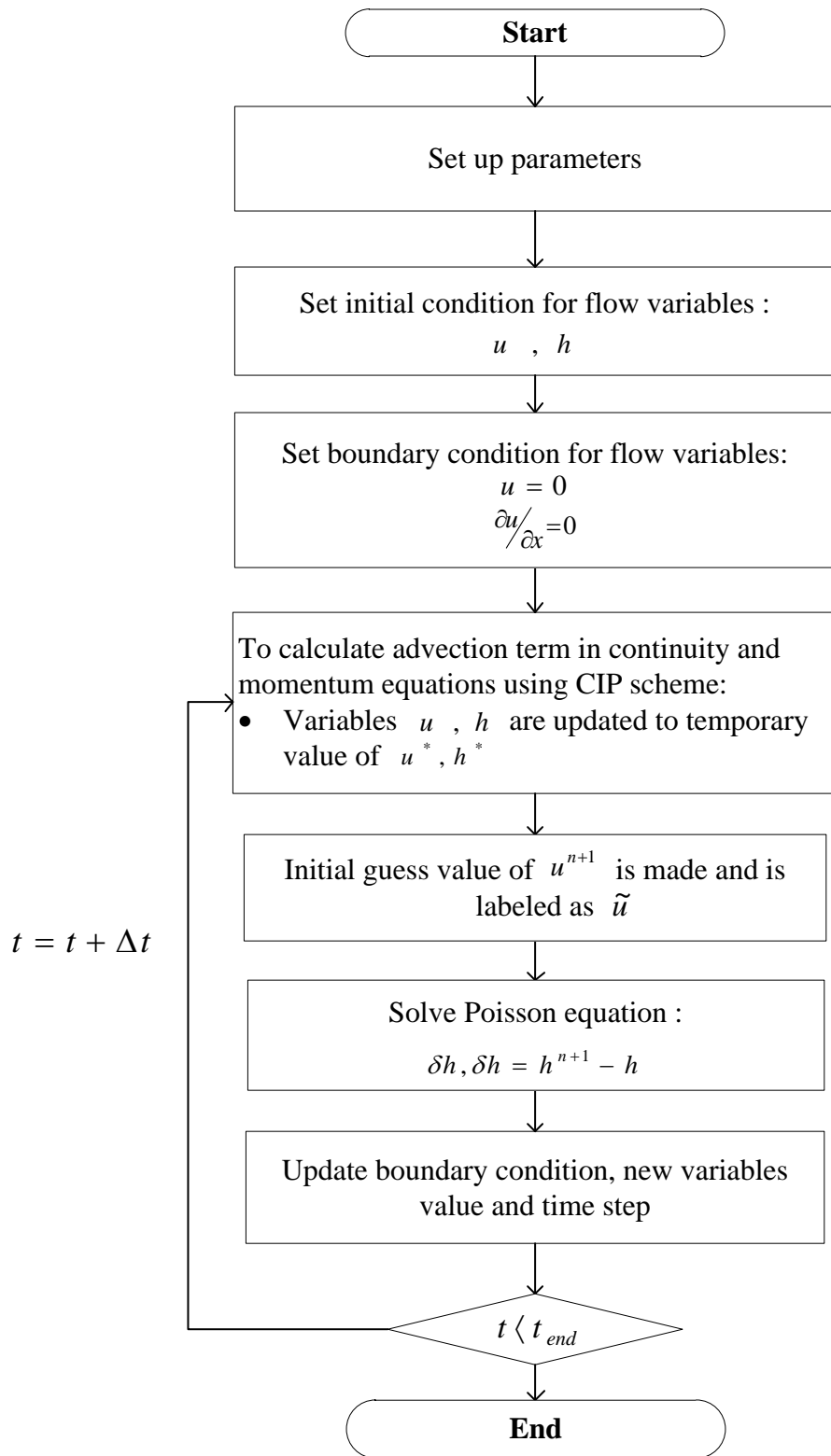


Figure 3-2: Solution algorithm for numerical model.